Supporting Information

Hierarchical self-assembly of a radical naphthalenediimide-based N-heterocyclic carbene-Au(I) macrocycle

Chong Wang,‡[a] Qing-Wen Zhu,‡[a] Jian-Gang Yu,[b] Xin Li,[a] Hao Li,[a] Li-Ying Sun[a] and Ying-Feng Han*[a]

[a]Key Laboratory of Synthetic and Natural Functional Molecule of the Ministry of Education, Xi'an Key Laboratory of Functional Supramolecular Structure and Materials, College of Chemistry and Materials Science, Northwest University, Xi'an 710127 (P. R. China).

[b]College of Chemical and Material Engineering, Quzhou University, Quzhou 324000 (P. R. China).

*Corresponding Authors: Prof. Y.-F. Han, E-mail: yfhan@nwu.edu.cn

‡ These authors contributed equally.

Table of Contents

1. Material and methods

All the synthetic experiments were performed using standard Schlenk techniques. Starting materials and reagents were AR grade quality, which were purchased from commercial sources and used without further purification unless otherwise noted. Compounds *anti*-atropisomer (*anti*-A)[1] and $^{n}Bu_4N[CuBr_2]$[2] were synthesized according to reported procedure. Column chromatography purification was performed in the air over silica gel (200-300 mesh). The ^{1}H and $^{13}C\{^{1}H\}$ and 2D NMR spectra were recorded on Bruker AVANCE III 400 and JEOL 400 spectrometers. Chemical shifts (δ) are expressed in ppm downfield from tetramethylsilane (TMS) using the residual protonated solvent peaks (^{1}H NMR: 2.50 ppm for DMSO-d_6; $^{13}C\{^{1}H\}$ NMR: 39.52 ppm for DMSO-d_6) as an internal standard. Mass spectra were obtained with a Bruker microTOF-Q II mass spectrometer (Bruker Daltonics Corp., USA) in the electrospray ionization (ESI) mode. Elemental analysis was conducted by an Elementar vario EL cube instrument. The UV-Vis experiments were conducted on an Agilent Cary-100 spectrophotometer. The continuous wave (CW) EPR spectra were obtained using an X-band Bruker E500 spectrometer at room temperature. The microwave frequency was 9.8 GHz and the modulation amplitude was 0.1 mT. All calculations were performed with the Gaussian(R) 09 program optimizer.[3] The theoretical approach is based on the framework of density functional theory (DFT).[4,5] The geometry optimizations were performed at B3LYP level using SDD basis set for Au element and the 6-31G* basis set for all of the other atoms. Multiwfn 3.8 was used to analyze the wave functions.[6]

2. Synthesis and characterization of compound $[H_2\text{-}1](BF_4)_2$

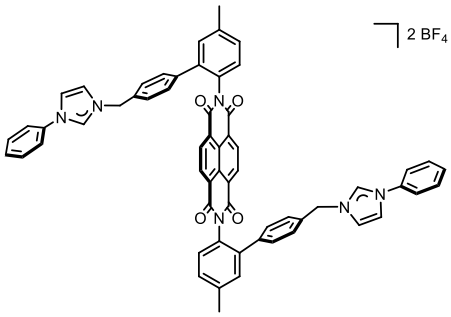

A 50 mL Schlenk flask was charged with *anti*-A (360 mg, 0.459 mmol) and 1-phenylimidazole (200 mg, 1.377 mmol). To this was added DMF (3 mL) and the reaction mixture was heated to 110°C for 24 h. The reaction mixture was cooled to ambient temperature, then ethyl acetate (30 mL) was added to the mixture and led to an orange precipitation. The solid was isolated by filtration and washed with ethyl acetate (3 × 5 mL) and dried *in vacuo*. The orange solid obtained was transferred to a bottle containing 10 mL methanol. Upon addition of a solution of NH_4BF_4 (192 mg, 1.836 mmol) in methanol (10 mL) to this solution, the tetrafluoroborate salt $[H_2\text{-}\mathbf{1}](BF_4)_2$ precipitated immediately. The precipitated solid was collected by filtration, washed with small portions of cold methanol and dried *in vacuo*. Yield: 446 mg (0.41 mmol, 89%). ^{1}H NMR (400 MHz, DMSO-d_6): δ = 9.83 (s, 1H, H1), 8.62 (s, 2H, H18), 8.27 (s, 1H, H2), 7.88 (s, 1H, H3), 7.75 – 7.71 (m, J = 8.4 Hz, 2H, H21), 7.64 (t, J = 7.3 Hz, 2H, H22), 7.59 (d, J = 6.8 Hz, 1H, H23), 7.41 (s, 2H, H13, H14), 7.36 – 7.26 (m, 5H, H6, H7, H10), 5.33 (s, 2H, H4), 2.46 (s, 3H, H12) ppm. ^{13}C{^{1}H} NMR (100 MHz, DMSO-d_6): δ = 162.9(C16), 139.4, 139.1, 139.0, 135.6(C1), 134.7, 133.8, 131.0, 130.3, 130.2, 129.9, 129.7, 129.5, 128.9, 128.4, 126.6(C3), 126.4(C20), 123.3(C3), 121.9, 121.7, 121.1, 51.9, 18.4 ppm. Elem. Anal. Calcd for $C_{60}H_{44}O_4N_6B_2F_8$, C 78.91, H 4.08, N 7.73; Found, C 78.86, H 4.05, N 7.70. HRMS (ESI, positive ions): m/z = 456.1836 (calcd for $[H_2\text{-}\mathbf{1}]^{2+}$ 456.1707).

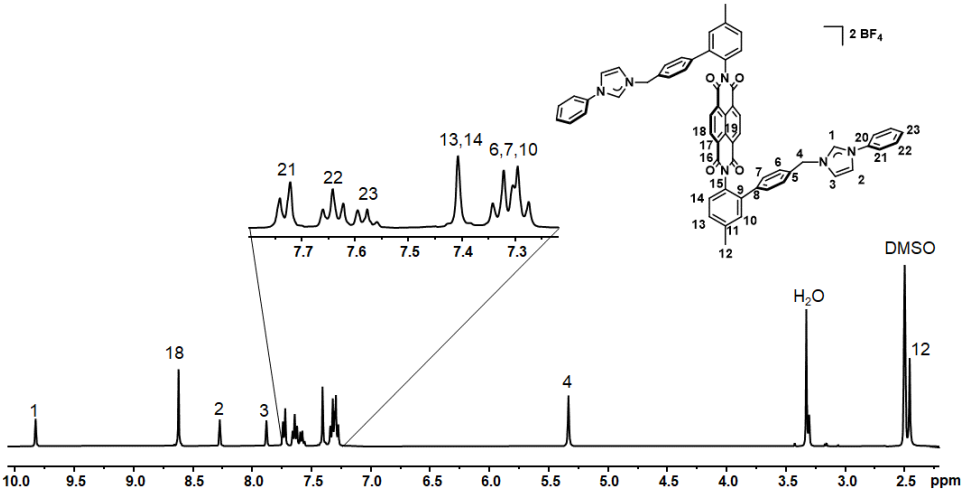

Figure S1. ^{1}H NMR spectrum of $[H_2\text{-}\mathbf{1}](BF_4)_2$ (400 MHz, DMSO-d_6).

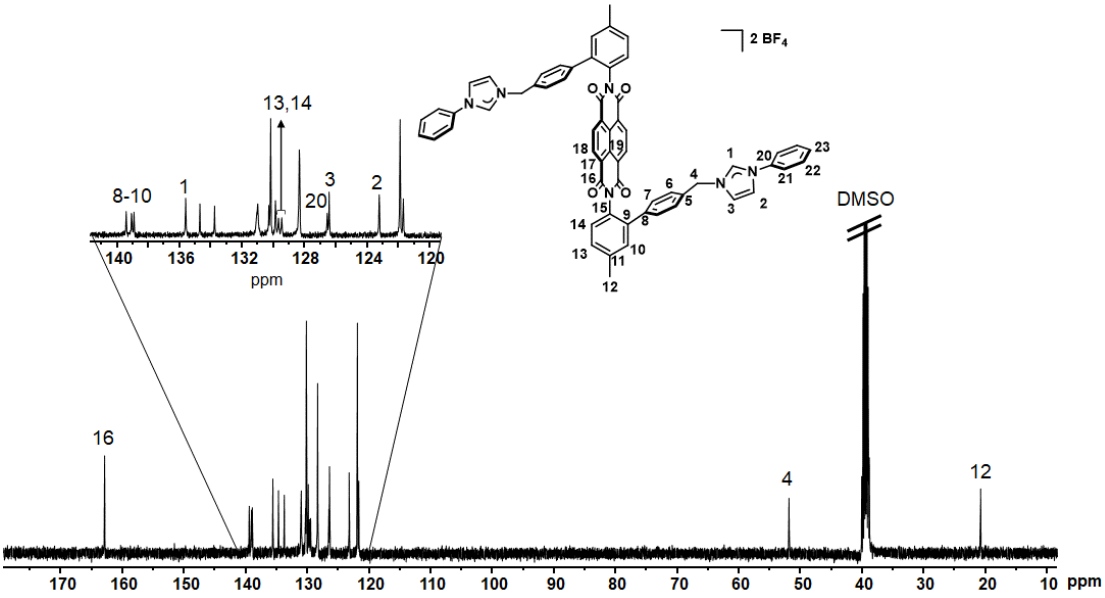

Figure S2. $^{13}C\{^{1}H\}$ NMR spectrum of $[H_2\text{-}\mathbf{1}](BF_4)_2$ (100 MHz, DMSO-d_6).

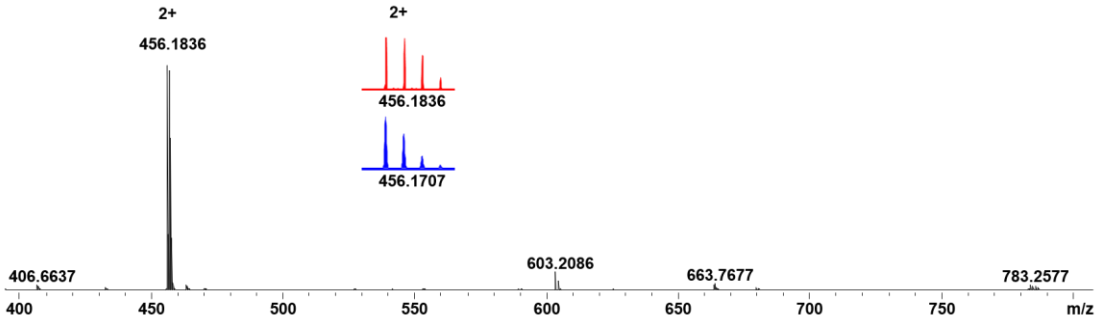

Figure S3. HR-ESI mass spectrum of $[H_2\text{-}\mathbf{1}](BF_4)_2$ with isotope distribution for selected peaks (experimental in red, calculated in blue).

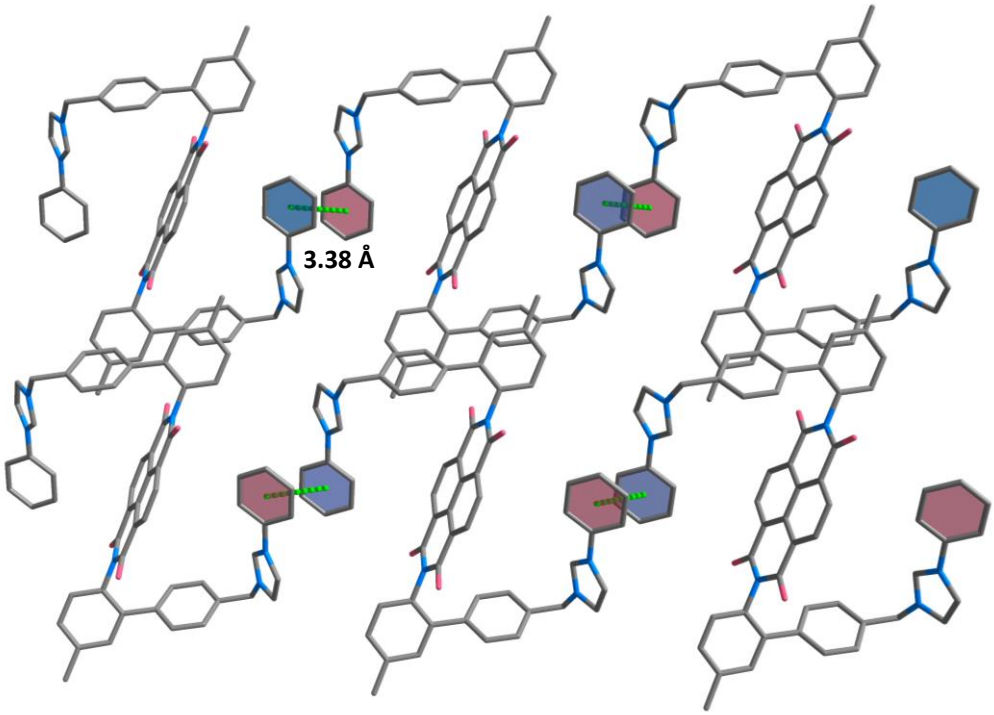

Figure S4. The packing motif of $[H_2\text{-}\mathbf{1}]^{2+}$. Hydrogen atoms and solvent molecules are omitted for the sake of clarity. Color scheme: C, gray; N, light blue; O, red.

3. Synthesis and characterization of complexes [M-1]BF_4 (M = Ag, Au).

3.1 Synthesis and characterization of complex [Ag-1]BF_4.

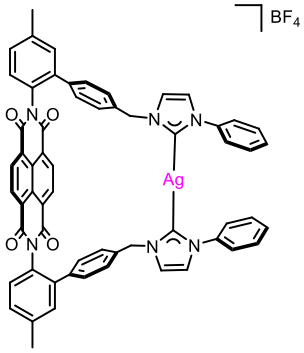

To a mixture of $[H_2\text{-}\mathbf{1}](BF_4)_2$ (100 mg, 0.092 mmol) and Ag_2O (48 mg, 0.184 mmol) was added 25 mL of acetonitrile. The reaction mixture was then heated to 70°C for 48 h under exclusion of light. After cooling to ambient temperature, the obtained suspension was filtered slowly through a short pad of Celite to obtain a clear solution. The filtrate was concentrated to 2 mL and ethyl acetate (30 mL) was added. A pale yellow precipitate formed, which was isolated by filtration, washed with diethyl ether and dried *in vacuo* to afford the complex [Ag-**1**]BF_4. Yield: 88 mg (0.079 mmol, 86%). ^{1}H NMR (400 MHz, DMSO-d_6): δ = 8.56 (s, 2H, H18), 7.79 (s, 1H, H2), 7.57 (s, 2H, H3), 7.52 (d, J = 2.0 Hz, 1H, H23), 7.46 (d, J = 8.0 Hz, 1H, H14), 7.43 – 7.39 (m, 3H, H10, H13), 7.33 (s, 1H, H21), 7.16 (d, J = 8.0 Hz, 2H, H7), 7.02 (d, J = 8.0 Hz, 2H, H6), 5.23 (s, 2H, H4), 2.46 (s, 3H, H12) ppm. ^{13}C{^{1}H} NMR (100 MHz, DMSO-d_6): δ = 178.5(C1),

171.6, 162.9(C16), 139.6, 139.4, 139.0, 138.4, 135.7(C5), 131.0, 130.8, 130.2, 129.6(C13), 129.3, 128.7, 128.2, 127.9, 126.3(C17), 123.9(C14), 123.2(C2), 122.6(C3), 59.1, 53.8(C4), 24.4(C12) ppm. Elem. Anal. Calcd for $C_{60}H_{42}O_4N_6AgBF_4$, C 65.09, H 3.80, N 7.60; Found, C 64.95, H 3.75, N 7.55. HRMS (ESI, positive ions): *m/z* = 1019.2207 (calcd for [Ag-**1**]$^+$ 1019.2313).

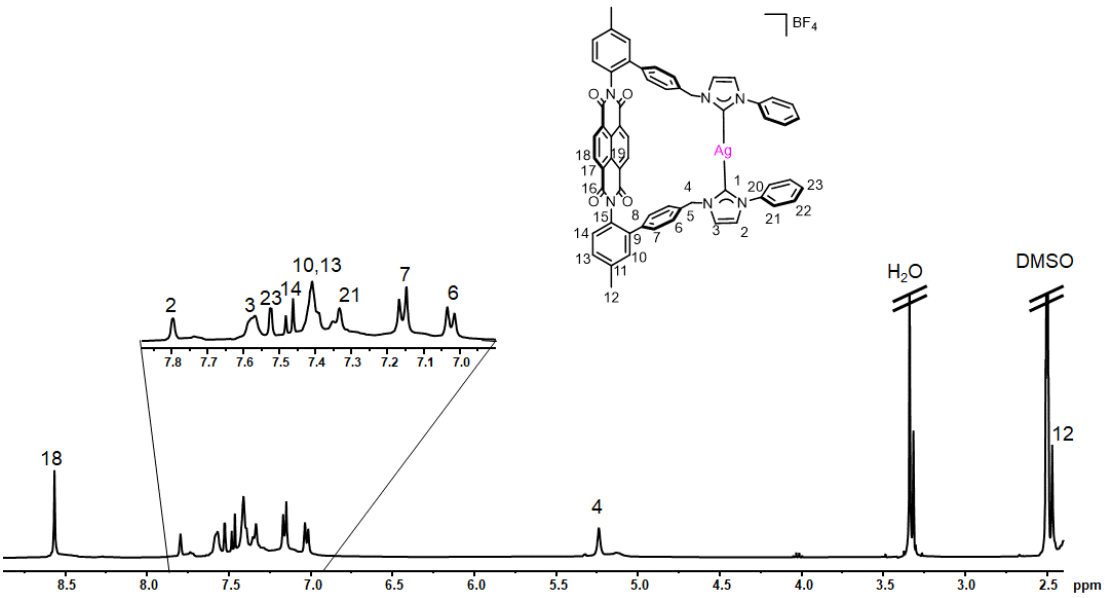

Figure S5. ^{1}H NMR spectrum of [Ag-**1**]BF_4 (400 MHz, DMSO-d_6).

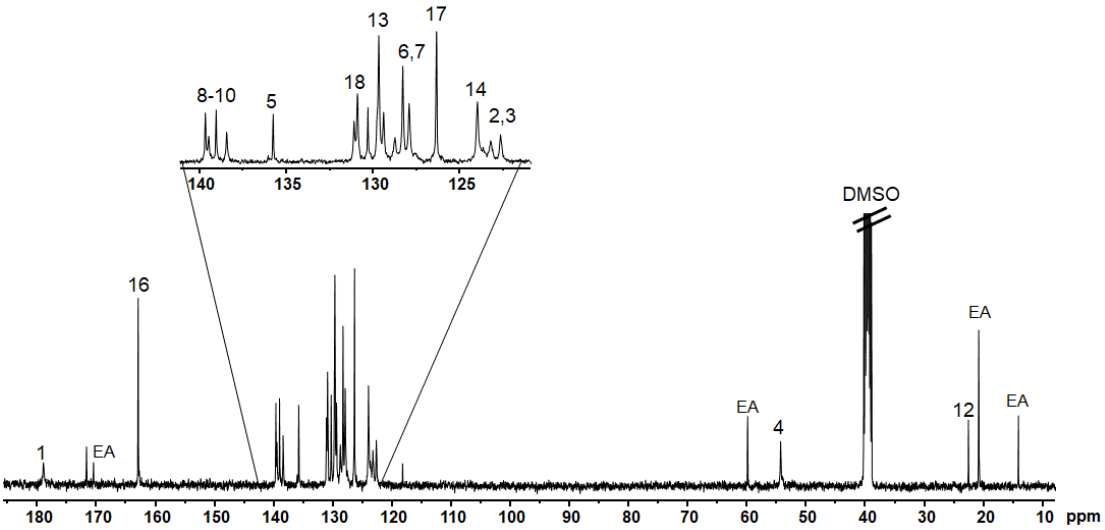

Figure S6. $^{13}C\{^1H\}$ NMR spectrum of [Ag-**1**]BF_4 (100 MHz, DMSO-d_6).

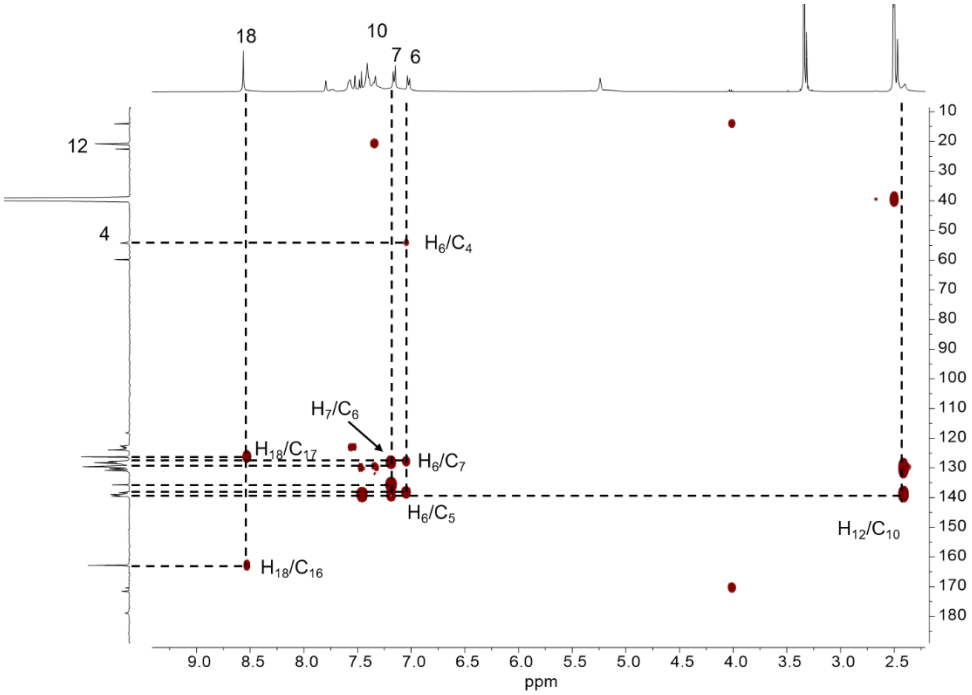

Figure S7. ^{1}H-^{13}C HMBC NMR spectrum of [Ag-**1**]BF_4 (400 MHz, DMSO-d_6).

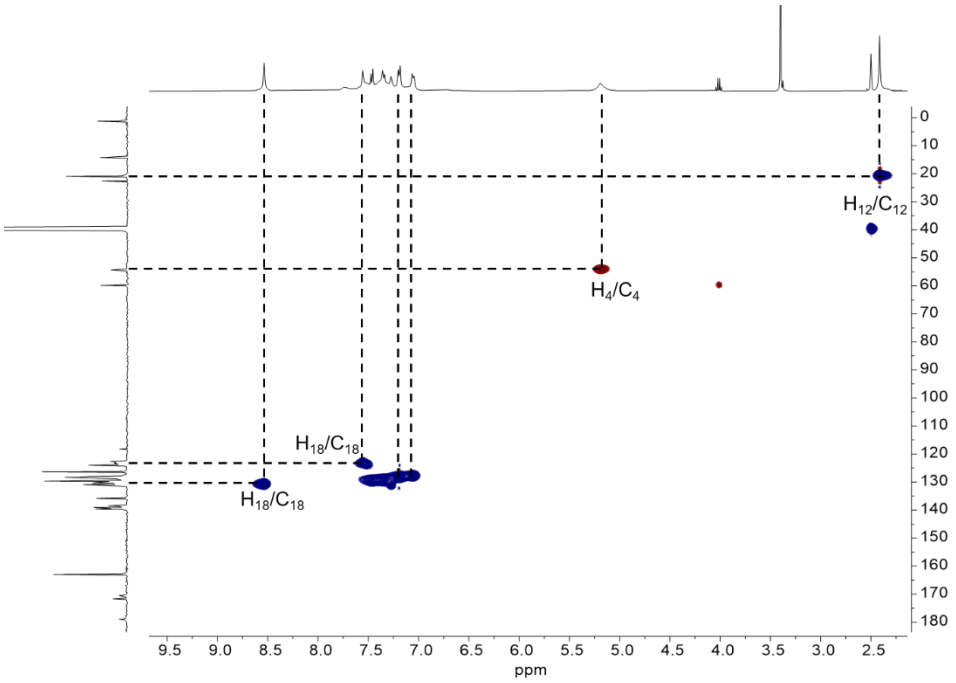

Figure S8. ^{1}H-^{13}C HSQC NMR spectrum of [Ag-**1**]BF_4 (400 MHz, DMSO-d_6).

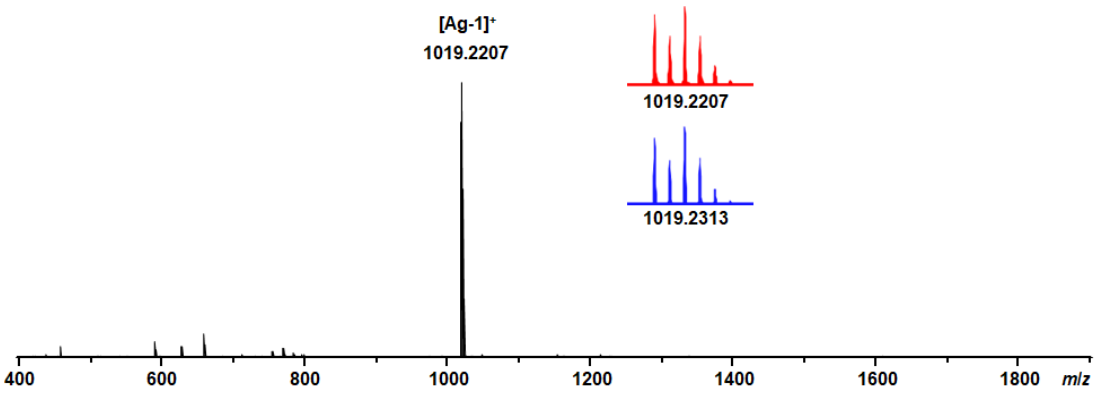

Figure S9. HR-ESI mass spectrum of [Ag-**1**]BF_4 with isotope distribution for selected peaks (experimental in red, calculated in blue).

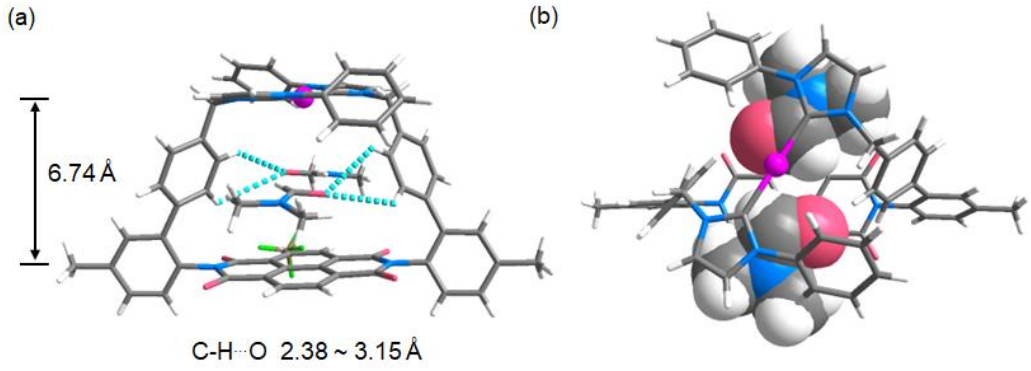

Figure S10. (a) Orientation of the diethyl ether molecules (sticks model) trapped inside the hollow cavity of [Ag-**1**]$^+$. (b) Orientation of the two dimethyl formamide molecules (space-filling model) trapped inside the hollow cavity of cation [Ag-**1**]$^+$. Color scheme: C, gray; H, white; N, light blue; O, red; Ag, pink; B, dark yellow; F, bright green.

3.2 Synthesis and characterization of complex [Au-1]BF_4.

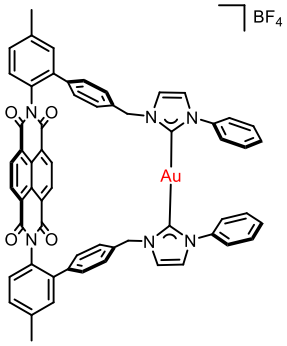

A solution of [Ag-**1**]BF_4 (160 mg, 0.145 mmol) in acetonitrile (25 mL) was added solid [AuCl(THT)] (65 mg, 0.202 mmol). Immediately after the addition the mixture turned from light yellow to dark purple. The reaction mixture was stirred at ambient temperature for 24 h and was then slowly filtered through a pad of Celite until a clear light yellow filtrate was obtained. The filtrate was concentrated to 1 mL and diethyl ether (30 mL) was added. A pale yellow precipitate formed, which was isolated by filtration, washed with diethyl ether and dried *in vacuo* to afford the complex [Au-**1**]BF_4. Yield: 142 mg (0.123 mmol, 82%). ^{1}H NMR (400 MHz, DMSO-d_6): δ = 8.55 (s, 2H, H18),

7.77 (s, 1H, H2), 7.71 (s, 1H,H3), 7.55 (d, J = 7.2 Hz, 2H, H13, H14), 7.49 – 7.43 (m, 3H, H10, H22, H23), 7.36 – 7.28 (m, 2H, H21), 7.14 (d, J = 7.6 Hz, 2H, H7), 6.92 (d, J = 8.0 Hz, 2H, H6), 5.19 (s, 2H, H4), 2.46 (s, 3H, H12) ppm. $^{13}C\{^{1}H\}$ NMR (100 MHz, DMSO-d_6): δ = 180.3(C1), 162.9(C16), 139.0, 138.7, 137.9, 135.0(C5), 131.0, 130.8(C18), 130.1, 129.8, 129.3(C13), 128.8, 128.2, 128.1, 127.6, 126.2, 125.1, 124.0(C2), 122.0(C3), 51.3, 8.3 ppm. Elem. Anal. Calcd for $C_{60}H_{42}O_4N_6AuBF_4$, C 60.29, H 3.54, N 7.03; Found, C 60.17, H 3.50, N 6.98. HRMS (ESI, positive ions): m/z = 1107.2862 (calcd for [Au-**1**]$^+$ 1107.2928).

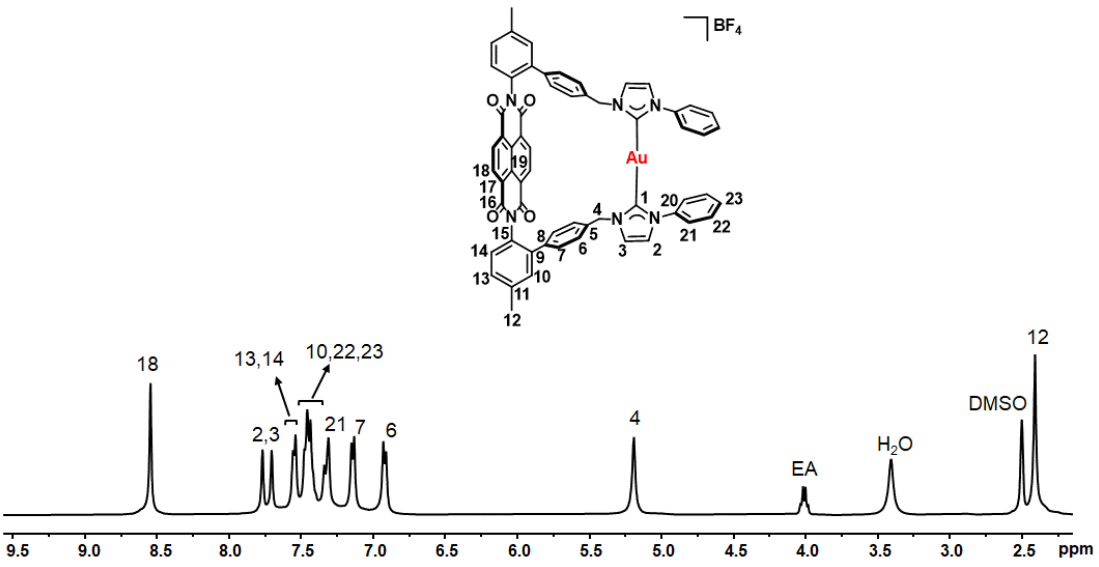

Figure S11. ^{1}H NMR spectrum of [Au-**1**]BF_4 (400 MHz, DMSO-d_6).

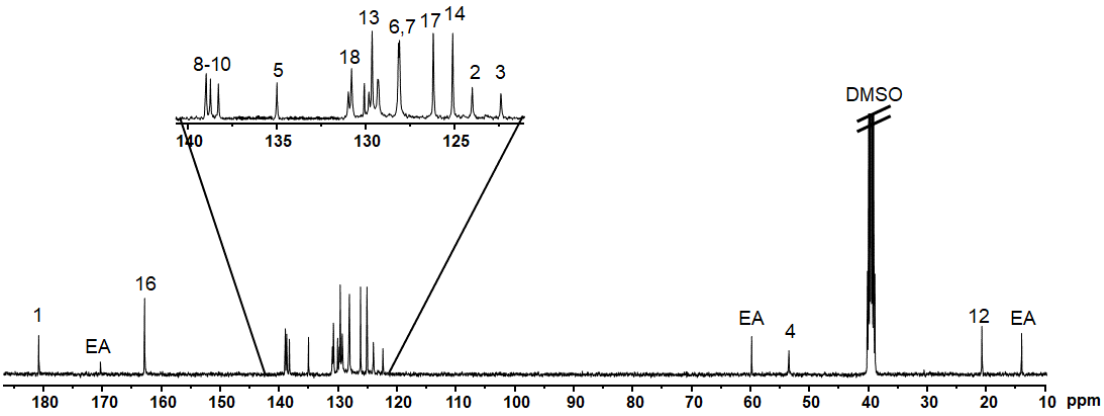

Figure S12. $^{13}C\{^{1}H\}$ NMR spectrum of [Au-**1**]BF_4 (100 MHz, DMSO-d_6).

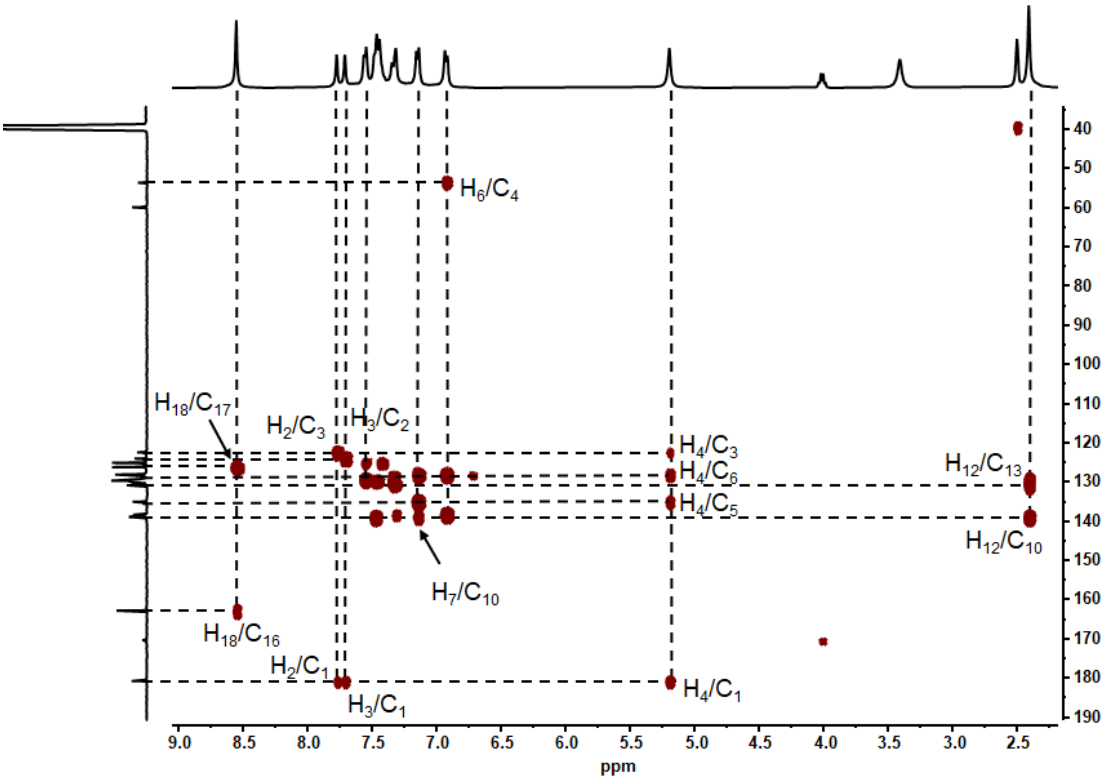

Figure S13. ^{1}H-^{13}C HMBC NMR spectrum of [Au-**1**]BF_4 (400 MHz, DMSO-d_6).

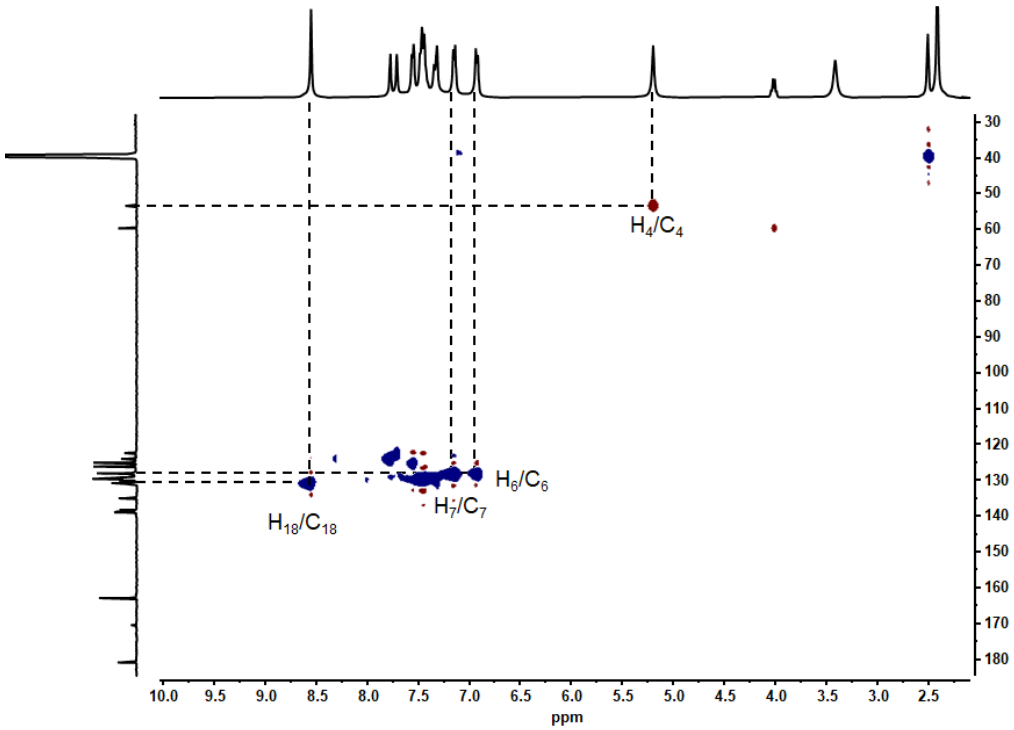

Figure S14. ^{1}H-^{13}C HSQC NMR spectrum of [Au-**1**]BF_4 (400 MHz, DMSO-d_6).

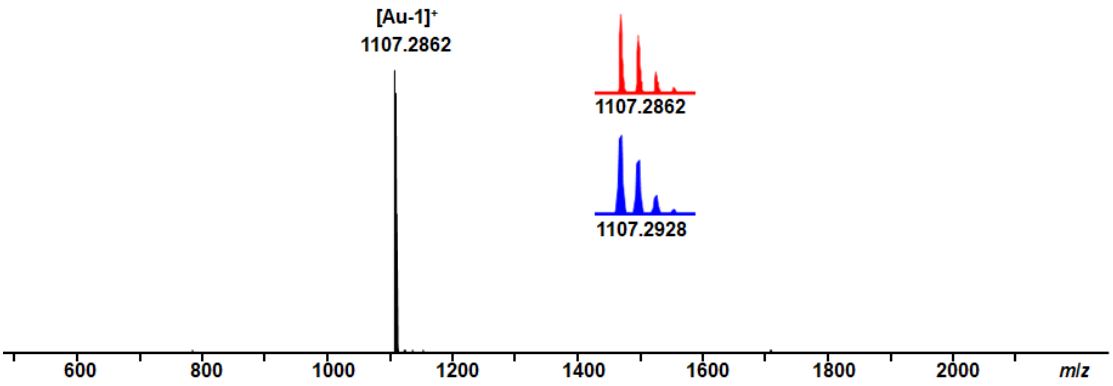

Figure S15. HR-ESI mass spectrum of [Au-**1**]BF_4 with isotope distribution for selected peaks (experimental in red, calculated in blue).

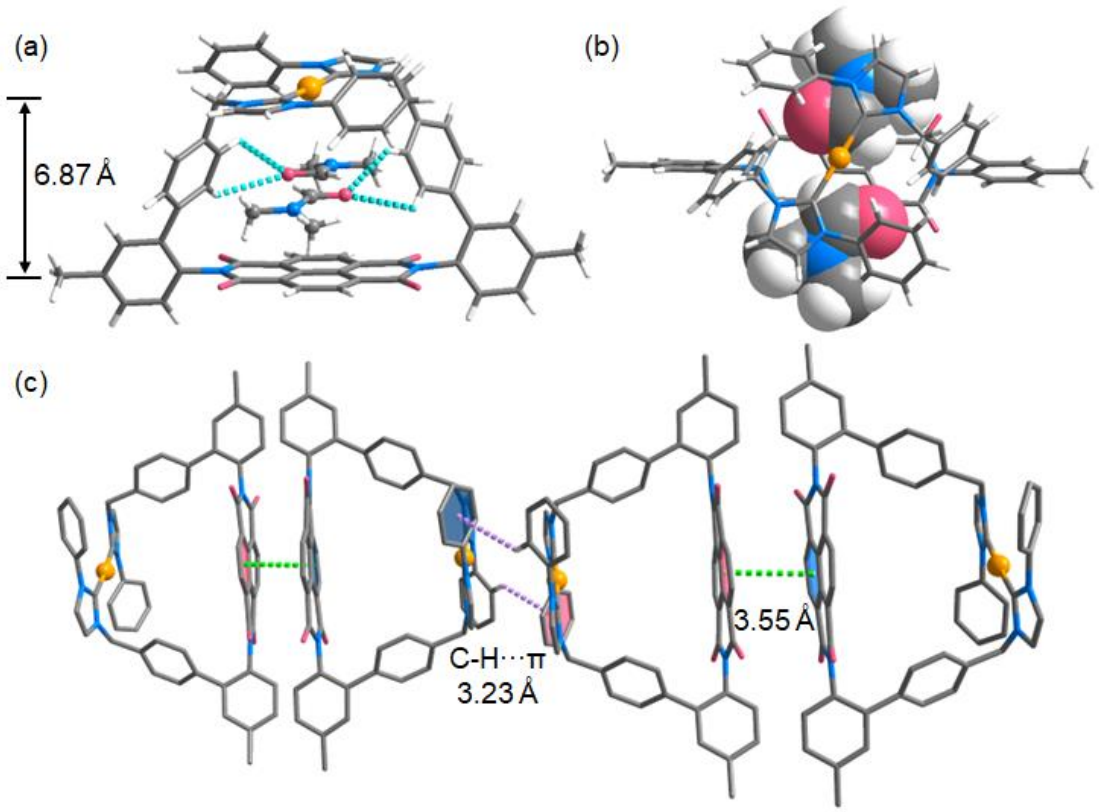

Figure S16. (a) Orientation of the DMF molecules (sticks model) trapped inside the hollow cavity of α-[Au-**1**]$^+$. (b) Orientation of the DMF molecules (space-filling model) trapped inside the hollow cavity of cation α-[Au-**1**]$^+$. (c) The crystal-packing diagram of α-[Au-**1**]$^+$. Color scheme: C, gray; N, light blue; O, red; Au, light orange.

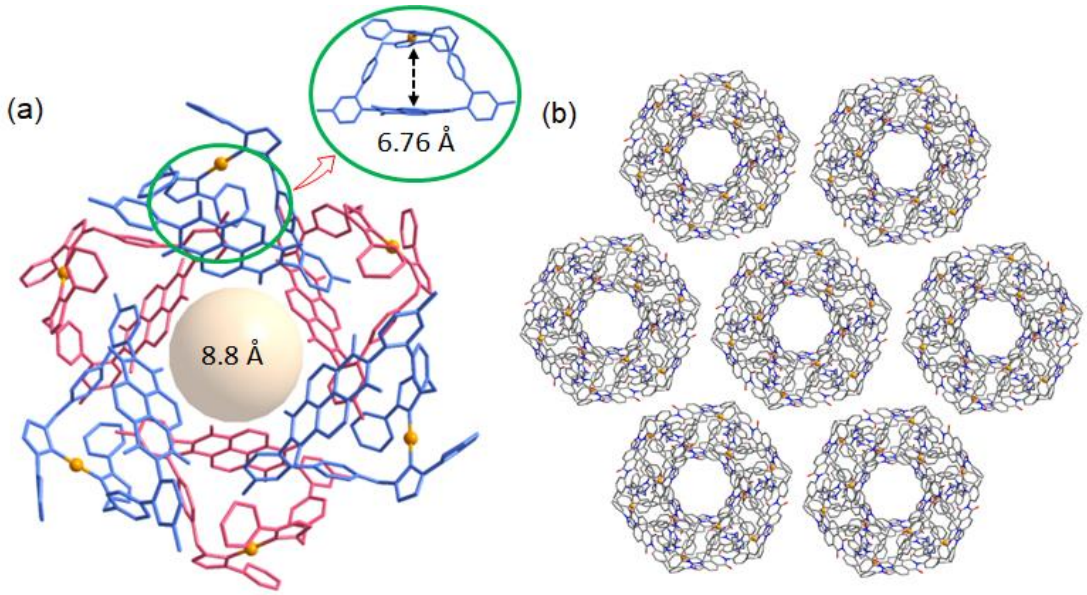

Figure S17. (a) Hexamer of NHC-Au(I) complex *β*-[Au-**1**]BF_4. (b) The crystal-packing diagram of *β*-[Au-**1**]BF_4. Hydrogen atoms and anions are omitted for clarity.

4. Synthesis and characterization of complex salt [Au-1][$CuBr_2$]

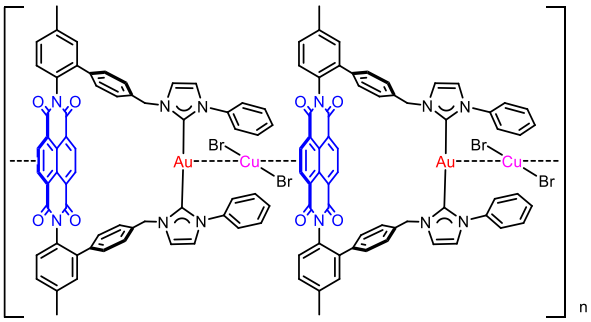

[Au-**1**]BF_4 (20 mg, 0.017 mmol) dissolved in acetonitrile (1.5 mL) and $^{n}Bu_4N[CuBr_2]$ (10 mg, 0.022 mmol) dissolved in acetonitrile (0.5 mL) were mixed, and an emissive solid precipitated in a few seconds. The precipitate was filtered after stirring for 10 min and washed thoroughly with water and acetonitrile, dried in air to give [Au-**1**][$CuBr_2$] as a gray solid (10 mg, yield: 44%). The crystalline powder solid was subject to powder X-ray diffraction measurement. HRMS (ESI, positive ions): *m/z* = 1107.2862 (calcd for $[Au\text{-}\mathbf{1}]^+$ 1107.2928); HRMS (ESI, negative ions): *m/z* = 222.7747 (calcd for $[CuBr_2]^-$ 222.7648).

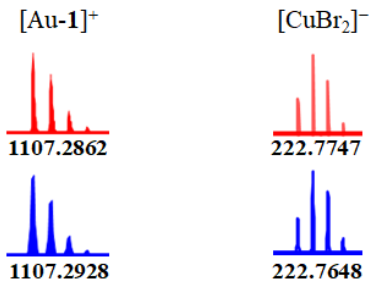

Figure S18. HR-ESI mass spectrum of [Au-**1**][$CuBr_2$] with isotope distribution for selected peaks (experimental in red, calculated in blue).

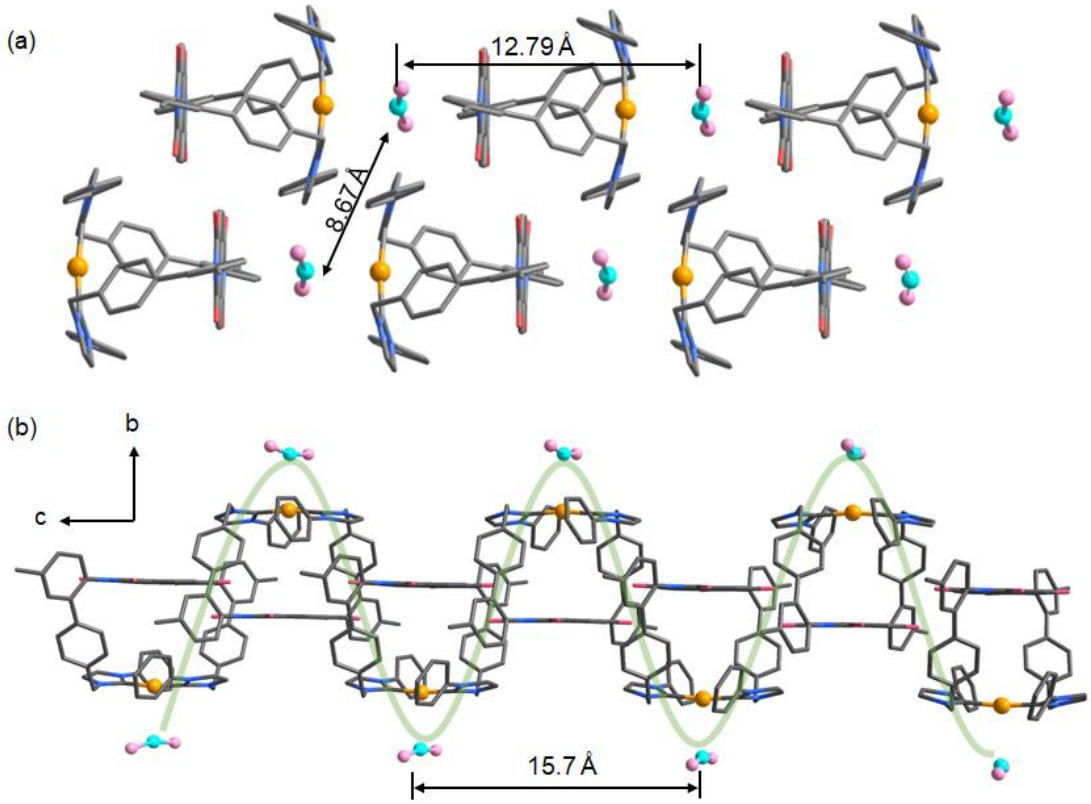

Figure S19. Packing diagrams of the single crystal structures of [Au-**1**][$CuBr_2$]. Color scheme: C, gray; N, light blue; O, red; Au, light orange; Cu, turquoise; Br, rose.

5. Crystallization protocols

5.1 Co-crystallization of [Au-1]BF_4 with pyrene

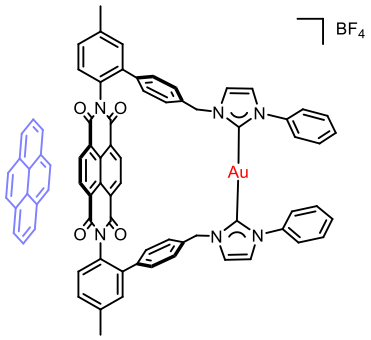

[Au-**1**]BF_4 (20 mg, 0.017 mmol) and pyrene (10 mg, 0.05 mmol) were dissolved in DMF (1.0 mL) to afford a red solution. After stirring the solution overnight, diethyl ether was diffused slowly into the DMF solution to afford red crystals (Pyr-[Au-**1**]BF_4) suitable for crystallographic studies.

5.2 Co-crystallization of [Au-1]BF_4 with naphthalene

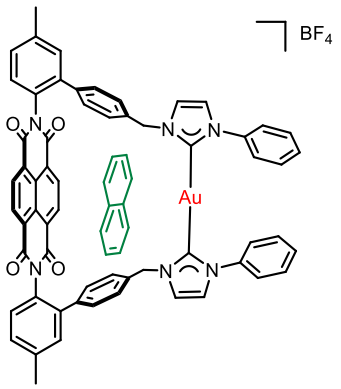

[Au-**1**]BF_4 (20 mg, 0.017 mmol) and naphthalene (10 mg, 0.078 mmol) were dissolved in MeCN (1.0 mL) to afford a dark green solution. After stirring the solution overnight, diethyl ether was diffused slowly into the MeCN solution to afford green crystals (Nap⊂[Au-**1**]BF_4) suitable for crystallographic studies.

^{1}H NMR titration experiments were performed in order to determine the binding affinity of [Au-**1**]BF_4 by adding increasing amounts of naphthalene to a CD_3CN solution of [Au-**1**]BF_4. Upon the consecutive addition of the solution of naphthalene, the signal assigned to the proton of the NDI core shifts upfield gradually. Then, the association constants (K) were calculated to be 16 ± 2.27 M^{-1} by nonlinear least-square analysis using the online software Bindfit.

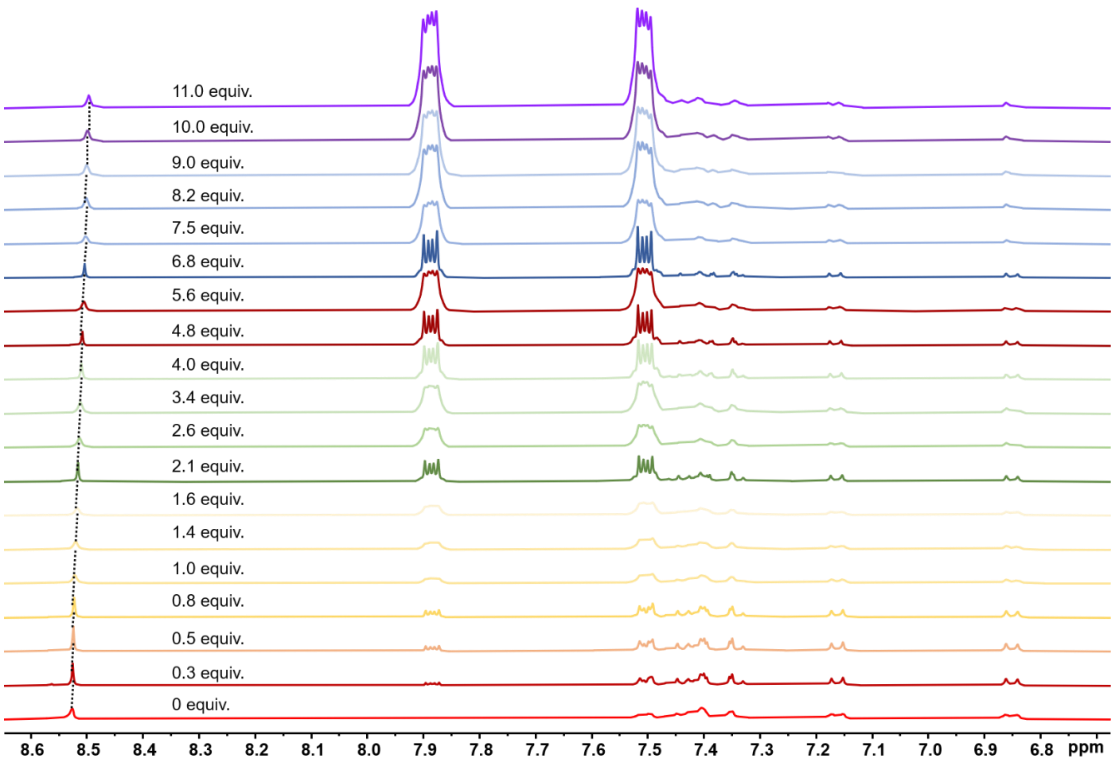

Figure S20 A stacked plot of the ^{1}H NMR titration (400 MHz, 298 K) of naphthalene into a solution of [Au-**1**]BF_4 in CD_3CN (c = 0.75 mM).

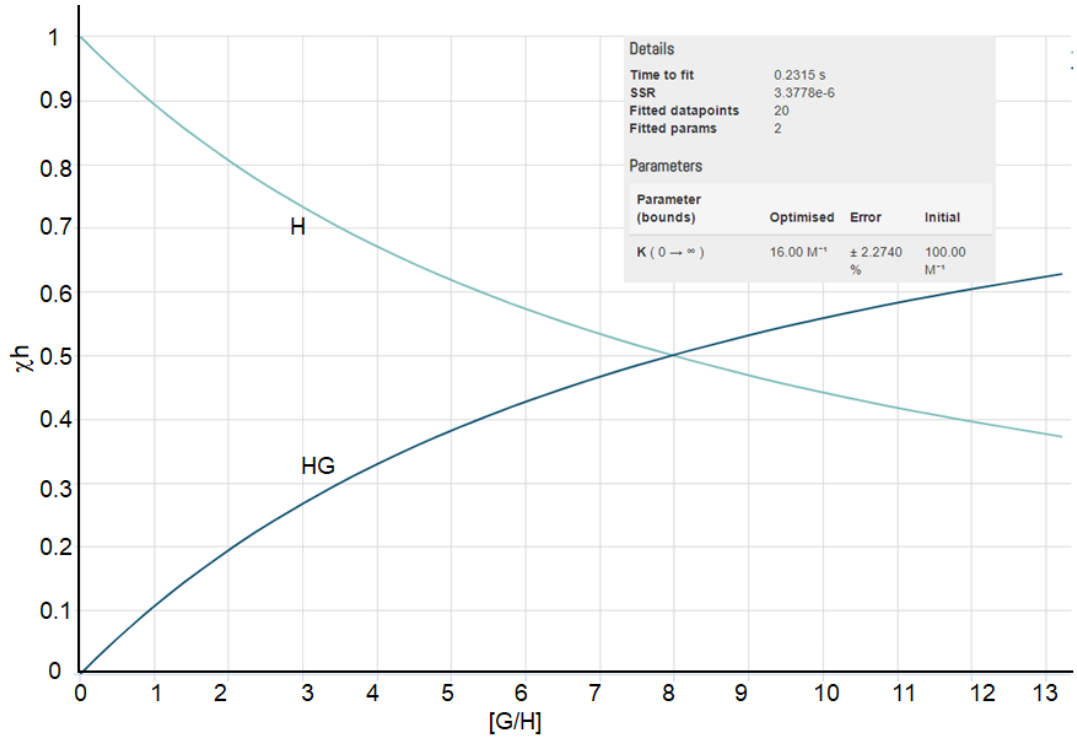

Figure S21 Non-linear least-squares fitting of the chemical shift changes of NDI-protons during titration experiments of [Au-**1**]BF_4 with naphthalene.

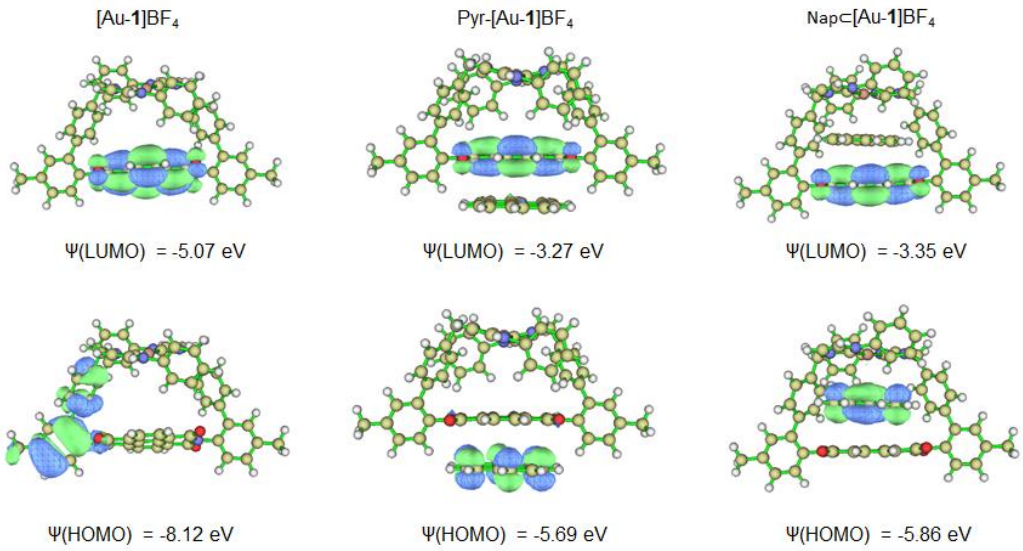

Figure S22. The calculated energy diagrams and molecular orbital diagrams of [Au-**1**]BF_4, Pyr-[Au-**1**]BF_4 and Nap⊂[Au-**1**]BF_4.

6. Electrochemical studies of $[H_2$-1$](BF_4)_2$ and [Au-1]BF_4

Cyclic voltammetry (CV) and differential pulse voltammetry (DPV) experiments were carried out using a CHI660E electrochemical workstation (CH Instruments, Inc). All CV experiments were performed using a glassy carbon working electrode (0.071 cm^2). The electrode surface was polished routinely with 0.05 μm alumina-water slurry on a felt surface immediately before use. The counter electrode was a platinum wire and the reference electrode was an Ag/AgCl electrode. All experiments were carried out under an atmosphere of argon in degassed and anhydrous acetonitrile solution containing [^{n}Bu_4N]PF_6 (0.1 M) at a scan rate of 100 mV s^{-1}.

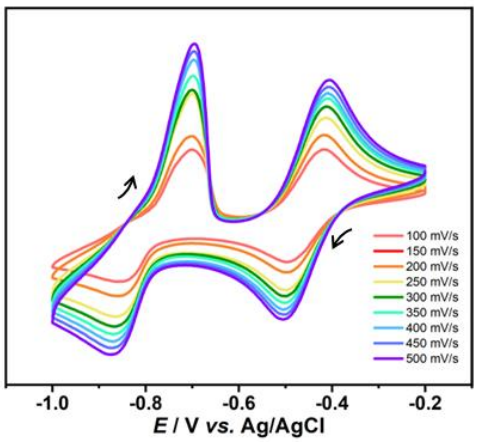

Figure S23. Cyclic voltammograms of $[H_2$-**1**$](BF_4)_2$ at different scan rates in CH_3CN.

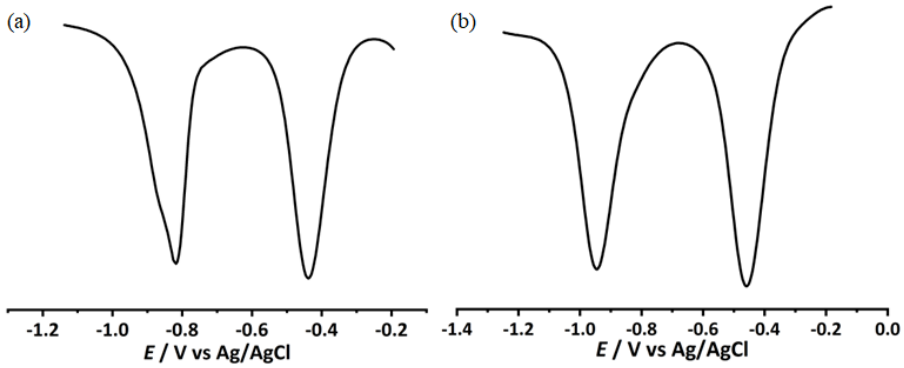

Figure S24. Differential pulse voltammogram of (a) [H_2-**1**]$(BF_4)_2$ and (b) [Au-**1**]BF_4. All the experiments were performed at 25°C in Ar-purged MeCN solution (c = 10^{-4} M) with 0.1 M [^{n}Bu_4N]PF_6 as the supporting electrolyte.

7. Formation and characterization of radical anion [Au-1]$^{\bullet}$

$CoCp_2$ (5 mg, 0.037 mmol) was added to a MeCN (2.0 mL) solution of [Au-**1**]BF_4 (20 mg, 0.017 mmol) at ambient temperature. The reaction mixture was further stirred for 5 h. Filtration through a plug of Celite afforded a brown black solution. diethyl ether was diffused slowly into the clear solution to afford dark crystals suitable for crystallographic studies. Elem. Anal. Calcd for $C_{60}H_{42}O_4N_6Au$, C 65.02, H 3.82, N 7.59; Found, C 64.85, H 3.66, N 7.50.

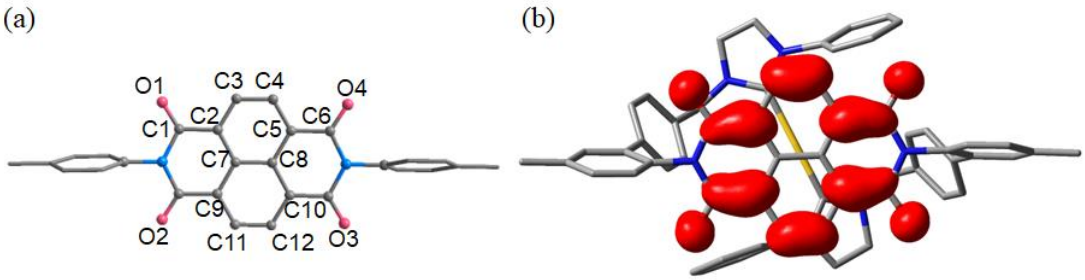

Figure S25. (a) Atomic number on NDI skeleton. (b) Spin density calculation of [Au-**1**]$^{\bullet}$.

8. NMR monitoring of redox process

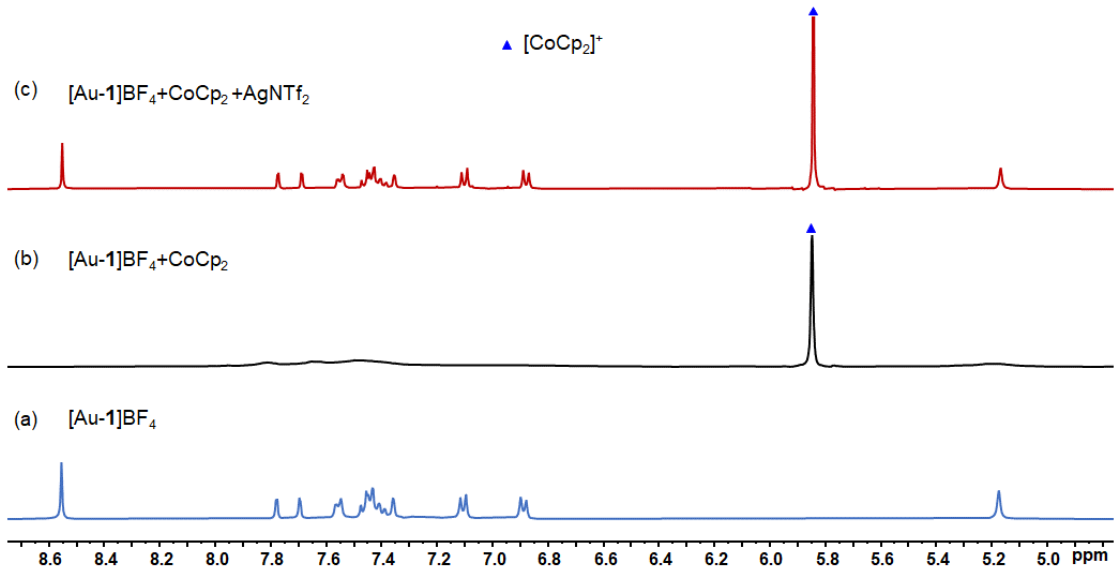

Figure S26. Sections of the ^{1}H NMR spectra (400 MHz, DMSO-d_6, 298 K) of (a) [Au-**1**]BF_4, (b) [Au-**1**]BF_4+ $CoCp_2$ (1.0 equiv.) and (c) [Au-**1**]BF_4+ $CoCp_2$ (1.0 equiv.)+ $AgNTf_2$ (1.2 equiv.).

9. X-ray crystallography

The crystals of all the compounds were selected for single-crystal X-ray diffraction. All data for crystal structure determinations were collected with a Bruker APEX-II CCD diffractometer. Reduction of data and semiempirical absorption correction were done using SADABS program. The structures were solved by direct methods, which revealed the position of all non-hydrogen atoms. These atoms were refined on F^2 by a full matrix least-squares procedure using anisotropic displacement parameters.[7] All hydrogen atoms were assigned to ideal positions and refined using a riding model. A number of disordered solvent molecules could not be restrained properly and were therefore removed using the SQUEEZE route.

Table S1. Crystal and refinement data for $[H_2\text{-}\mathbf{1}]Br_2$.

Empirical formula	$C_{66}H_{58}Br_2N_8O_6$
Formula weight	1219.02
Temperature (K)	150
Crystal system	monoclinic
Space group	$P2_1/c$
a (Å)	14.1932(12)
b (Å)	13.1909(9)
c (Å)	16.8635(14)
α (°)	90
β (°)	113.991(3)
γ (°)	90
Volume (Å^3)	2884.3(4)
Z	2
ρ_{calc} (g·cm^{-3})	1.404
μ (mm^{-1})	1.466
F(000)	1256.0
Crystal size (mm^3)	0.21 × 0.2 × 0.2
Radiation	Mo Kα (λ = 0.71073)
2θ range for data collection (°)	4.432 to 50.666
Index ranges	17 ≥ h ≥ -17, 15 ≥ k ≥ -15, 20 ≥ l ≥ -2
Reflections collected	27449
Independent reflections	5216 [R_{int} = 0.0667, R_{sigma} = 0.0524]
Data/restraints/parameters	5216/32/373
Goodness-of-fit on F^2	1.054
Final R indexes [I ≥ 2σ (I)]	R_1 = 0.0868, wR_2 = 0.2446
Final R indexes [all data]	R_1 = 0.1107, wR_2 = 0.2667
Largest diff. peak/hole (e Å^{-3})	0.76/-1.54
CCDC	2225597

Table S2. Crystal and refinement data for [Ag-**1**]BF_4.

Empirical formula	$C_{148}H_{147}Ag_2B_2F_8N_{20}O_{17}$
Formula weight	2867.21
Temperature/K	150
Crystal system	triclinic
Space group	$P\bar{1}$
a/Å	18.8525(10)
b/Å	20.5694(10)
c/Å	20.6759(11)
α/°	63.2750(10)
β/°	79.415(2)
γ/°	71.5460(10)
Volume/Å^3	6785.0(6)
Z	2
ρ_{calc}g/cm^3	1.403
μ/mm^{-1}	0.374
F(000)	2974.0
Crystal size/mm^3	0.2 × 0.2 × 0.19
Radiation	Mo Kα (λ = 0.71073)
2Θ range for data collection/°	4.486 to 50.11
Index ranges	-22 ≤ h ≤ 22, -24 ≤ k ≤ 24, -24 ≤ l ≤ 24
Reflections collected	93596
Independent reflections	23953 [R_{int} = 0.0944, R_{sigma} = 0.0939]
Data/restraints/parameters	23953/248/1796
Goodness-of-fit on F^2	1.035
Final R indexes [I>=2σ (I)]	R_1 = 0.0734, wR_2 = 0.1835
Final R indexes [all data]	R_1 = 0.1383, wR_2 = 0.2203
Largest diff. peak/hole / e Å^{-3}	1.85/-0.75
CCDC	2225599

Table S3. Crystal and refinement data for α-[Au-**1**]BF_4.

Empirical formula	$C_{72}H_{70}Au_2BF_4N_{10}O_8$
Formula weight	1487.15
Temperature/K	180
Crystal system	triclinic
Space group	$P\bar{1}$
a/Å	18.8792(7)
b/Å	20.6936(8)
c/Å	20.9007(9)
α/°	62.8430(10)
β/°	80.4630(10)
γ/°	70.4420(10)
Volume/Å^3	6845.3(5)
Z	4
ρ_{calc}g/cm^3	1.443
μ/mm^{-1}	2.223
F(000)	3024.0
Crystal size/mm^3	0.23 × 0.22 × 0.21
Radiation	Mo Kα (λ = 0.71073)
2Θ range for data collection/°	4.632 to 50.728
Index ranges	-22 ≤ h ≤ 22, -24 ≤ k ≤ 24, -25 ≤ l ≤ 25
Reflections collected	130391
Independent reflections	25016 [R_{int} = 0.0289, R_{sigma} = 0.0221]
Data/restraints/parameters	25016/256/1787
Goodness-of-fit on F^2	1.018
Final R indexes [I>=2σ (I)]	R_1 = 0.0340, wR_2 = 0.0875
Final R indexes [all data]	R_1 = 0.0417, wR_2 = 0.0920
Largest diff. peak/hole / e Å^{-3}	1.69/-1.09
CCDC	2225600

Table S4. Crystal and refinement data for β-[Au-**1**]BF_4.

Empirical formula	$C_{60}H_{42}AuBF_4N_6O_4$
Formula weight	1194.77
Temperature/K	180
Crystal system	trigonal
Space group	$R\bar{3}$
a/Å	32.0842(14)
b/Å	32.0842(14)
c/Å	32.4821(16)
α/°	90
β/°	90
γ/°	120
Volume/Å^3	28957(3)
Z	1
ρ_{calc}g/cm^3	1.233
μ/mm^{-1}	3.347
F(000)	10728.0
Crystal size/mm^3	0.23 × 0.22 × 0.21
Radiation	Ga Kα (λ = 1.34139)
2Θ range for data collection/°	3.64 to 113.9
Index ranges	-24 ≤ h ≤ 21, -34 ≤ k ≤ 40, -40 ≤ l ≤ 35
Reflections collected	48908
Independent reflections	12982 [R_{int} = 0.0388, R_{sigma} = 0.0343]
Data/restraints/parameters	12982/267/606
Goodness-of-fit on F^2	1.079
Final R indexes [I>=2σ (I)]	R_1 = 0.0692, wR_2 = 0.2070
Final R indexes [all data]	R_1 = 0.0840, wR_2 = 0.2187
Largest diff. peak/hole / e Å^{-3}	1.66/-2.03
CCDC	2225601

Table S5. Crystal and refinement data for [Au-**1**][$CuBr_2$].

Empirical formula	$C_{60}H_{44}AuBr_2CuN_6O_4$
Formula weight	1333.94
Temperature/K	180
Crystal system	monoclinic
Space group	*P*2/*c*
a/Å	15.6670(14)
b/Å	12.7990(11)
c/Å	15.7277(14)
α/°	90
β/°	101.677(3)
γ/°	90
Volume/Å^3	3088.5(5)
Z	2
ρ_{calc}g/cm^3	1.434
μ/mm^{-1}	4.057
F(000)	1312.0
Crystal size/mm^3	0.23 × 0.22 × 0.21
Radiation	Mo Kα (λ = 0.71073)
2Θ range for data collection/°	5.198 to 50.812
Index ranges	-18 ≤ h ≤ 18, -14 ≤ k ≤ 15, -18 ≤ l ≤ 18
Reflections collected	27255
Independent reflections	5676 [R_{int} = 0.0579, R_{sigma} = 0.0492]
Data/restraints/parameters	5676/63/279
Goodness-of-fit on F^2	1.115
Final *R* indexes [I>=2σ (I)]	R_1 = 0.0808, wR_2 = 0.1918
Final *R* indexes [all data]	R_1 = 0.0965, wR_2 = 0.1990
Largest diff. peak/hole / e Å^{-3}	3.52/-2.34
CCDC	2225602

Table S6. Crystal and refinement data for Pyr-[Au-**1**]BF_4

Empirical formula	$C_{79}H_{58}AuBF_4N_7O_5\cdot(H_2O)_{0.5}$
Formula weight	1478.10
Temperature/K	220
Crystal system	monoclinic
Space group	*P*21/*n*
a/Å	11.2997(3)
b/Å	26.5107(7)
c/Å	23.5697(8)
α/°	90
β/°	91.4860(10)
γ/°	90
Volume/Å^3	7058.2(4)
Z	4
ρ_{calc}g/cm^3	1.391
μ/mm^{-1}	2.152
F(000)	2984.0
Crystal size/mm^3	0.2 × 0.14 × 0.12
Radiation	Mo Kα (λ = 0.71073)
2Θ range for data collection/°	3.784 to 50.748
Index ranges	-13 ≤ h ≤ 13, -30 ≤ k ≤ 31, -28 ≤ l ≤ 28
Reflections collected	41778
Independent reflections	12921 [R_{int} = 0.0575, R_{sigma} = 0.0666]
Data/restraints/parameters	12912/124/881
Goodness-of-fit on F^2	1.035
Final *R* indexes [*I*>=2σ (I)]	R_1 = 0.0539, wR_2 = 0.1485
Final *R* indexes [all data]	*R*1 = 0.0971, wR_2 = 0.1749
Largest diff. peak/hole / e Å^{-3}	1.07/-0.60
CCDC	2225603

Table S7. Crystal and refinement data for Nap⊂[Au-**1**]BF_4

Empirical formula	$C_{153}H_{116}Au_2B_2F_8N_{16}O_8$
Formula weight	2874.16
Temperature/K	230
Crystal system	triclinic
Space group	$P\bar{1}$
a/Å	15.991(4)
b/Å	21.435(6)
c/Å	21.946(5)
α/°	89.388(8)
β/°	76.692(8)
γ/°	70.171(8)
Volume/Å^3	6868(3)
Z	2
ρ_{calc}g/cm^3	1.390
μ/mm^{-1}	2.208
F(000)	2900.0
Crystal size/mm^3	0.12 × 0.09 × 0.06
Radiation	Mo Kα (λ = 0.71073)
2Θ range for data collection/°	3.742 to 50.204
Index ranges	-19 ≤ h ≤ 18, -25 ≤ k ≤ 25, -23 ≤ l ≤ 26
Reflections collected	100952
Independent reflections	24110 [R_{int} = 0.0886, R_{sigma} = 0.0859]
Data/restraints/parameters	24110/213/1710
Goodness-of-fit on F^2	1.017
Final R indexes [I>=2σ (I)]	R_1 = 0.0635, wR_2 = 0.1630
Final R indexes [all data]	R_1 = 0.1087, wR_2 = 0.1889
Largest diff. peak/hole / e Å^{-3}	1.90/-1.27
CCDC	2225604

Table S7. Crystal and refinement data for [Au-**1**]$^{\bullet}$

Empirical formula	$C_{60}H_{42}AuN_6O_4$
Formula weight	1107.96
Temperature/K	220
Crystal system	monoclinic
Space group	*C2/c*
a/Å	20.1490(17)
b/Å	9.3955(7)
c/Å	26.588(2)
α/°	90
β/°	90.208(2)
γ/°	90
Volume/Å^3	5033.4(7)
Z	4
ρ_{calc}g/cm^3	1.462
μ/mm^{-1}	2.977
F(000)	2220.0
Crystal size/mm^3	0.15 × 0.1 × 0.08
Radiation	Mo Kα (λ = 0.71073)
2Θ range for data collection/°	5.02 to 52.782
Index ranges	-25 ≤ h ≤ 25, -11 ≤ k ≤ 11, -33 ≤ l ≤ 27
Reflections collected	14263
Independent reflections	5125 [R_{int} = 0.0642, R_{sigma} = 0.0863]
Data/restraints/parameters	5125/0/322
Goodness-of-fit on F^2	1.042
Final *R* indexes [*I*>=2σ (I)]	R_1 = 0.0534, wR_2 = 0.1269
Final *R* indexes [all data]	R_1 = 0.0909, wR_2 = 0.1429
Largest diff. peak/hole / e Å^{-3}	1.32/-1.19
CCDC	2225605

10. References

1. F. Yang, C.-P. Liu, D. Yin, Y.-Q. Xu, M.-Y. Wu and W. Wei, Atropisomer-based construction of macrocyclic hosts that selectively recognize tryptophan from standard amino acids, *Chem. Commun.*, **2019**, *55*, 14335−14338.

2. Q. Liu, M. Xie, X. Y. Chang, S. Cao, C. Zou, W.-F. Fu, C.-M. Che, Y. Chen and W. Lu, Tunable Multicolor Phosphorescence of Crystalline Polymeric Complex Salts with Metallophilic Backbones, *Angew. Chem. Int. Ed.*, **2018**, *57*, 6279−6283.

3. M. J. Frisch, G. W. Trucks, H. B. Schlegel, G. E. Scuseria, M. A. Robb, J. R. Cheeseman, G. Scalmani, V. Barone, B. Mennucci, G. A. Petersson, H. Nakatsuji, M. Caricato, X. Li, H. P. Hratchian, A. F. Izmaylov, J. Bloino, G. Zheng, J. L. Sonnenberg, M. Hada, M. Ehara, K. Toyota, R. Fukuda, J. Hasegawa, M. Ishida, T. Nakajima, Y. Honda, O. Kitao, H. Nakai, T. Vreven, J. J. A. Montgomery, J. E. Peralta, F. Ogliaro, M. Bearpark, J. J. Heyd, E. Brothers, K. N. Kudin, V. N. Staroverov, R. Kobayashi, J. Normand, K. Raghavachari, A. Rendell, J. C. Burant, S. S. Iyengar, J. Tomasi, M. Cossi, N. Rega, J. M. Millam, M. Klene, J. E. Knox, J. B. Cross, V. Bakken, C. Adamo, J. Jaramillo, R. Gomperts, R. E. Stratmann, O. Yazyev, A. J. Austin, R. Cammi, C. Pomelli, J. W. Ochterski, R. L. Martin, K. Morokuma, V. G. Zakrzewski, G. A. Voth, P. Salvador, J. J. Dannenberg, S. Dapprich, A. D. Daniels, O. Farkas, J. B. Foresman, J. V. Ortiz, J. Cioslowski, D. J. Fox, Gaussian, Inc., Revision E.01. Wallingford CT, **2013**.

4. P. Hohenberg and W. Kohn, Inhomogeneous Electron Gas, *Phys. Rev. B.*, **1964**, *136*, B864−B871.

5. W. Kohn and L. Sham, Self-Consistent Equations Including Exchange and Correlation Effects, *J. Phys. Rev.*, **1965**, *140*, A1133−A1138.

6. T. Lu and F. Chen, Multiwfn: A multifunctional wavefunction analyzer, *J. Comput. Chem.*, **2012**, *33*, 580–592.

7. (a) L. J. Bourhis, O. V. Dolomanov, R. J. Gildea, J. A. K. Howard, H. Puschmann, The anatomy of a comprehensive constrained, restrained refinement program for the modern computing environment – Olex2 dissected, *Acta Crystallogr., Sect. A,* **2015**, *71*, 59–75; (b) G. M. Sheldrick, Crystal structure refinement with SHELXL, *Acta Crystallogr., Sect. C,* **2015**, *71*, 3–8.